

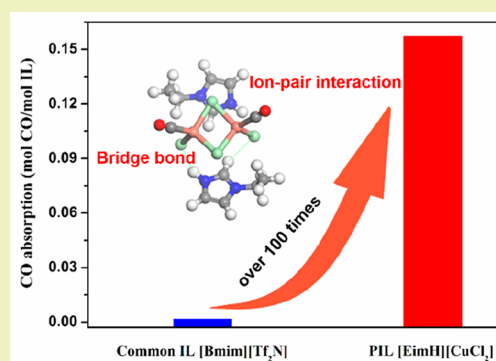
Tuning Ion-Pair Interaction in Cuprous-Based Protic Ionic Liquids for Significantly Improved CO Capture

Yu-Mei Liu,^{†,‡} Ziqi Tian,^{‡,†} Feng Qu,[†] Yan Zhou,[†] Yong Liu,[§] and Duan-Jian Tao^{*,†}[†]College of Chemistry and Chemical Engineering, Jiangxi Normal University, Nanchang 330022, China[‡]Ningbo Institute of Materials Technology & Engineering, Chinese Academy of Sciences, Ningbo, Zhejiang 315201, China[§]Henan Key Laboratory of Polyoxometalate, College of Chemistry and Chemical Engineering, Henan University, Kaifeng 475004, China

Supporting Information

ABSTRACT: Because of the high bond dissociation energy of CO, achieving efficient absorption of CO in liquid solvents is still a significant challenge in gas separation. Herein, it is unprecedentedly found that cuprous-based protic ionic liquid (PIL) [EimH][CuCl₂] exhibits ultrahigh absorption capacity for CO, with the value of 0.157 mol·mol⁻¹ at 293.2 K and 1 bar, being 100 times that of a commonly used IL [Bmim][Tf₂N] (0.0015 mol·mol⁻¹). The IR and Raman spectroscopies coupled with theoretical calculation demonstrated that the protonated imidazolium cation ([EimH]⁺) played an essential role in strengthening the ion–pair interaction between CO and dinuclear cuprous species, contributing to an obvious red shift for the system [EimH][CuCl₂] + CO and thereby to such superior CO capacity. Furthermore, the PIL [EimH][CuCl₂] displayed very large absorption selectivities for CO/CO₂, CO/N₂, and CO/H₂, and the absorption of CO was completely reversible. The present work thus triggers important guidance for the design of new solvents with promising application in selective separation of CO.

KEYWORDS: CO capture, Protic ionic liquids, Chlorocuprate, Ion–pair interaction, Selective absorption



INTRODUCTION

The emission of carbon monoxide (CO) in fuel combustion causes damage to human health because of its high hemoglobin affinity. On the other hand, CO in industrial syngas is also an important resource to develop C₁ chemistry, in which a variety of major chemical products including methanol, aldehydes, carboxylic acid, and amide can be produced. Therefore, research into the removal and purification of CO is important in fields involving the environment and the chemical industry.^{1–4} Generally, the technologies for separation and purification of CO include ammoniacal cuprous chloride, aromatic CuAlCl₄ solution (COSORB),⁵ pressure swing adsorption (PSA), and cryogenic fractionation-supported liquid membranes (SLMs).⁶ However, these methods have several inherent drawbacks such as low capture capacity, emission of volatile organic compounds (VOCs), and harsh operating conditions. Therefore, novel sorbents and functional materials are still constantly and highly demanded for efficient CO capture.

In recent years, ionic liquids (ILs) have attracted considerable attention owing to their distinct advantages including extremely low volatility, excellent solubility, high thermal stability, and virtually unlimited tunability. Thus, ILs have been proved to be efficient absorbents for many gases, such as CO₂,^{7–9} SO₂,^{10,11} H₂S,¹² NO_x,¹³ and NH₃.¹⁴ However,

there are a limited number of studies concerning the capture of CO by ILs.^{15–18} For example, Laurency and co-workers reported their pioneering work on physical absorption of CO by an IL ([Bmim][Tf₂N]) in 2004, in which a solubility of 1.25 × 10⁻³ mol mol⁻¹ was achieved at ambient pressure.¹⁵ After that, other functionalized ILs were also explored for CO capture, including [hmim][CuCl₂] and [P₄₄₄₈][Pen].^{19,20}

Indeed, CO can behave as a π-acid and readily coordinate with d-block transition metals through a CO-to-metal π-complexation. It is known that copper(I) could act as an efficient and optimum carrier for the capture of CO.²¹ However, an IL [hmim][CuCl₂] just exhibited a very low solubility of 0.02 mol of CO per mol of IL at ambient pressure,¹⁹ indicating that Cu⁺ in [hmim][CuCl₂] may be blocked and results in a poor activity to absorb CO. Recently, the subset of protic ionic liquids (PILs) has a number of unique properties and receives significant interest compared to other ILs.²² PILs can be easily synthesized via neutralization of Brønsted acids and bases.²³ The distinct feature of PILs is that the proton can enhance the hydrogen bond donor ability of the cations and the hydrogen bond acceptor ability of the anions,

Received: May 7, 2019

Revised: May 31, 2019

Published: June 3, 2019

which can build a strong hydrogen-bonding network and increase the capture ability of PILs.²⁴ Therefore, it is envisioned that the Cu⁺ ion in cuprous-based PILs is more likely to interact with CO efficiently and leads to a high CO capacity, which has never been explored to the best of our knowledge.

Herein, we conceived an efficient CO capture system based on a series of novel cuprous-based PILs of 1-alkylimidazolium chlorocuprate ([RimH][CuCl₂]), as shown in Figure 1. We

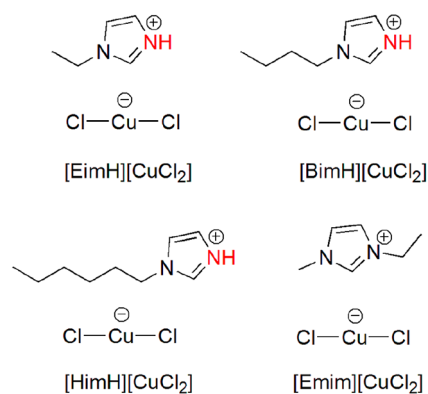


Figure 1. Structures of the anions and the cations in PILs.

show that these PILs are capable of reversibly capturing CO with an extremely high capacity (0.157 mol per mol of PIL) and display large absorption selectivities for CO/CO₂, CO/N₂, and CO/H₂. The IR and Raman spectroscopies coupled with theoretical calculation further demonstrated that the protonated imidazolium cation ([RimH]⁺) played an essential role in strengthening the ion–pair interaction between CO and dinuclear cuprous species, contributing to such superior CO capacity and high selectivity. In addition, the CO solubility of [EimH][CuCl₂] and its thermodynamic behavior were studied in detail.

EXPERIMENTAL SECTION

Materials. 1-Ethyl-3-methylimidazolium chloride ([Emim]Cl, 99%), 1-ethylimidazole hydrochloride ([EimH]Cl, 99%), 1-butylimidazole hydrochloride ([BimH]Cl, 99%), and 1-hexylimidazole hydrochloride ([HimH]Cl, 99%) were obtained from the Centre of Green Chemistry and Catalysis, LICP, CAS. Cuprous chloride (CuCl, 99.95%) was purchased from Adamas (Shanghai, Adamas-Beta). CO, CO₂, H₂, and N₂ with a purity of 99.99% were commercially available. All the other chemicals were obtained in the highest purity grade possible and used as received.

Preparation and Characterization of Cuprous-Based PILs. The novel cuprous-based PILs were prepared by simple mixing of imidazolium hydrochloride and cuprous salt. In a typical synthesis of 1-ethylimidazolium chlorocuprate ([EimH][CuCl₂]), equimolar [EimH]Cl was mixed with CuCl and then stirred at room temperature for 2 h. The obtained PIL [EimH][CuCl₂] was dried in high vacuum for 24 h at 333.2 K to remove possible traces of water. The synthesis procedure for the other two PILs [BimH][CuCl₂] and [HimH][CuCl₂] and aprotic IL [Emim][CuCl₂] was similar to that described in the preparation of [EimH][CuCl₂].

The cuprous-based PILs [EimH][CuCl₂], [BimH][CuCl₂], and [HimH][CuCl₂] were characterized by electrospray ionization mass spectrometry (ESI-MS) with positive and negative ion modes using an Agilent1290/maX impact instrument. The C, N, and H elemental analysis of cuprous-based PILs was carried out on an Elementar Vario El III. IR spectra were recorded on a NEXUS870 FT-IR spectrometer. The copper contents in the samples were determined by inductively

coupled plasma optical emission spectrometry (ICP-OES) using an Agilent 720 instrument after the sample was completely dissolved in the mixture of HNO₃/HCl (1:3 ratio). Raman spectra of cuprous-based PILs before and after the capture of CO were obtained in a LabRAM HR spectrometer with an excitation wavelength at 632 nm with 3 cm⁻¹ spectral resolution. An Anton Paar DMA4500 automatic densitometer and cone–plate viscometer (Brookfield DV II+Pro) were employed to measure the densities and viscosities of cuprous-based PILs, respectively, at 303.2 K with a temperature control of ±0.1 K. The precision of the density apparatus was ±0.001 g·cm⁻³, which was calibrated with dry air before each series of measurements. The thermal equilibrium time in the viscometer was about 0.5 h with a viscosity uncertainty of ±1%.

Measurement of CO Absorption. The device for measuring CO absorption consists of two parts: a gas storage chamber (the bigger cell) and an absorption chamber (the smaller cell), to our previous work on CO₂ and CO absorption.^{8,9,20} In a typical run, a known mass (*w*) of IL was placed in the absorption chamber, and the air in the two storages was evacuated. The pressure in the absorption chamber was recorded to be *P*₀. CO from the gas cylinder was then fed into the gas reservoir to a pressure of *P*₁. CO was introduced to the absorption chamber by the needle valve between the two chambers. Absorption equilibrium was reached when the pressures of the two chambers remained constant for at least 2 h. The equilibrium pressures were denoted as *P*₂ for the absorption chamber and *P*'₁ for the gas storage chamber. The CO partial pressure in the absorption chamber was *P*_S = *P*₂ - *P*₀. The CO uptake, *n*(*P*_S), can thus be calculated using the following equation

$$n(P_S) = \rho_g(P_i, T)V_1 - \rho_g(P'_1, T)V_1 - \rho_g(P_s, T)(V_2 - w/\rho_{IL}) \quad (1)$$

where $\rho_g(P_i, T)$ represents the density of CO in mol/cm³ at *P*_{*i*} (*i* = 1, S) and *T*. ρ_{IL} is the density of the ionic liquid in g/cm³ at *T*. *V*₁ and *V*₂ represent the volumes in cm³ of the two chambers, respectively. Continual determinations of solubility data at elevated pressures were performed by introducing more CO into the equilibrium cell to reach new equilibrium. The solubility of CO was defined in terms of mol of CO per mol of IL. Duplicate experiments were run for each IL to obtain averaged values of CO solubilities. The averaged uncertainty of the absorption data in this work was well within ±1%.

RESULTS AND DISCUSSION

Characterization and CO Absorption Capacities of PILs. These cuprous-based PILs [RimH][CuCl₂] were easily prepared by a mixture of 1-alkylimidazolium hydrochloride with CuCl. The structures of these PILs were verified by electrospray ionization mass spectrometry (ESI-MS), inductively coupled plasma optical emission spectrometry (ICP-OES), and CHN elemental analysis (Supporting Information, Figures S1–3). The water content of these PILs was determined with a Karl Fisher titration and found to be less than 0.1 wt %. The physical properties including glass transition temperature, density, and viscosity of these PILs were also measured, and the results are listed in Table S1 and Figure S4.

The solubilities of CO in these cuprous-based PILs were determined under ambient conditions (Table 1). To our delight, the PILs exhibited very high capacities for capturing CO at room temperature and atmospheric pressure. For example, for [EimH][CuCl₂], 0.118 mol of CO per mol of PIL was achieved at 303.2 K under ambient pressure, while [BimH][CuCl₂] and [HimH][CuCl₂] showed a CO capacity of 0.111 and 0.105 mol·mol⁻¹ at 303.2 K, respectively. This implies that the alkyl length of imidazolium-based PILs has little effect on their CO absorption capacities. Moreover, we further investigated the viscosity of the PIL [RimH][CuCl₂]

Table 1. Absorption Capacity of CO in Cuprous-Based PILs Compared with other ILs

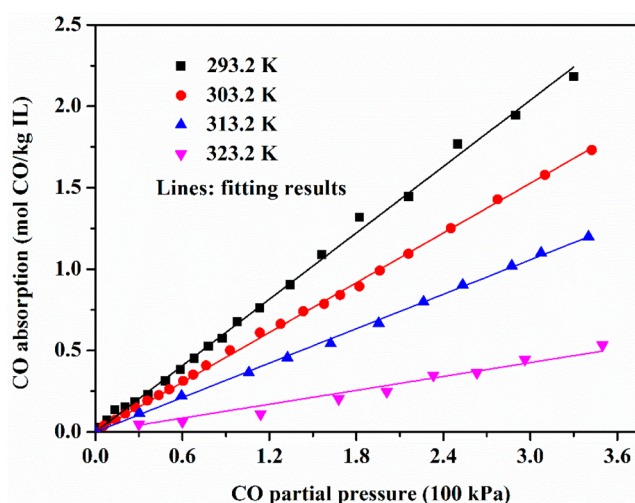
absorbent	temperature (K)	pressure (bar)	solubility (mol·mol ⁻¹)	ref
[EimH][CuCl ₂]	293.2	1.0	0.157	-
[EimH][CuCl ₂]	303.2	1.0	0.118	-
[Emim][CuCl ₂]	303.2	1.0	0.037	-
[BimH][CuCl ₂]	303.2	1.0	0.111	-
[HimH][CuCl ₂]	303.2	1.0	0.105	-
[Bmim][PF ₆]	295.2	1.0	3.0 × 10 ⁻³	15
[Bmim][Tf ₂ N]	303.2	1.0	1.5 × 10 ⁻³	18
[hmim][CuCl ₂]	303.2	1.0	0.020	19
[P ₄₄₄₈][Pen]	303.2	1.0	0.046	20

before and after CO capture. It can be seen from Table S1 that the viscosity of [EimH][CuCl₂] increased only slightly from 30 to 179 cP after CO absorption. However, the viscosity of the other PILs remarkably enhanced to 1655 and 3106 cP, respectively, after CO absorption. Therefore, [EimH][CuCl₂] can maintain good fluidity during the process of CO capture and thereby show a good potential in the industrial capture of CO.

For comparison, an aprotic IL [Emim][CuCl₂] was prepared and tested for capturing CO at various temperatures and pressures (Supporting Information, Figure S5). However, the CO solubility of [Emim][CuCl₂] was only 0.037 mol·mol⁻¹ at 303.2 K and 1 bar, which is much lower than [EimH][CuCl₂]. When the pressure increased to 3 bar, the absorption capacity of CO in [Emim][CuCl₂] was still significantly less than the performance of [EimH][CuCl₂]. This result speculates that compared with the imidazolium cation [Emim]⁺ the protonated imidazolium cation ([EimH]⁺) may play a key role in ultrahigh CO uptake. Moreover, the data from previous studies^{15–20} showed that most ILs and organic solvents had solubilities of no more than 0.05 mol mol⁻¹ (Table 1). To the best of our knowledge, it is clear that the PIL [EimH][CuCl₂] is significantly greater than most ILs and organic solvents in terms of CO uptake.

In addition, the effects of temperature and pressure on the capture of CO by [RimH][CuCl₂] were also tested (Supporting Information, Table S2). It is found that the CO absorption capacity of [EimH][CuCl₂] increased to 0.157 mol of CO per mol of IL when the temperature was decreased to 293.2 K, indicating that low temperature is favorable to CO capture, and it is also shown that the CO uptake of [EimH][CuCl₂] improved obviously, from 0.118 to 0.354 mol per mol of IL, when the partial pressure increased from 1 to 3 bar. High pressure is beneficial for the capture of CO, which is a common phenomenon for gas absorption in liquid solvents.^{8–13}

Thermodynamic Analysis of [EimH][CuCl₂] for Capturing CO. The absorption capacities of CO in the PIL [EimH][CuCl₂] was measured at temperatures from 293.2 to 323.2 K and pressures from 0.01 to 3.5 bar. The solubility data are graphically shown in Figure 2. It can be seen that the solubilities of CO in [EimH][CuCl₂] increased linearly with an increase of CO partial pressure. This means that these absorption isotherms at different temperatures show the typical physical absorption processes for [EimH][CuCl₂] capturing CO. The physical absorption of a gas in a solvent is frequently described as Henry's law

**Figure 2.** Absorption of CO in [EimH][CuCl₂] at different temperatures.

$$H_m(T, P) = \lim_{m_{\text{CO}} \rightarrow 0} \frac{f^{\text{g}}}{m_{\text{CO}}} \approx \frac{P}{m_{\text{CO}}} \quad (2)$$

where $H_m(T, P)$ is the Henry's law constant in terms of molality in 100 kPa·kg·mol⁻¹; m_{CO} is the molality of CO dissolved in the liquid phase in mol·kg⁻¹; f^{g} is the fugacity of CO in kPa; and P is the equilibrium CO partial pressure.

Therefore, the Henry constants H_m can be estimated according to experimental data with eq 2, and the values of H_m at 293.2–323.2 K are given in Table 2. It is shown that temperature increase causes the increase of H_m . As is known, a larger H_m corresponds to a lower absorption capacity. Therefore, a low temperature is favorable and a good choice for the absorption of CO.

The enthalpy of solution ΔH_{sol} can reflect the thermal effect of physical dissolution of CO in [EimH][CuCl₂]. By drawing a linear fit of $\ln H_m$ with $1/T$, ΔH_{sol} was then calculated from eq 3 and is graphically shown in Figure 3. In addition, the Gibbs energy of dissolution (ΔG_{sol}) and entropy of dissolution (ΔS_{sol}) also can be calculated by eq 4 and eq 5, respectively.

$$\frac{\partial \ln H_m}{\partial T} = -\frac{\Delta H_{\text{sol}}}{RT^2} \quad (3)$$

$$\Delta G_{\text{sol}} = -\frac{RT \ln(H_m(T, P))}{P^0} \quad (4)$$

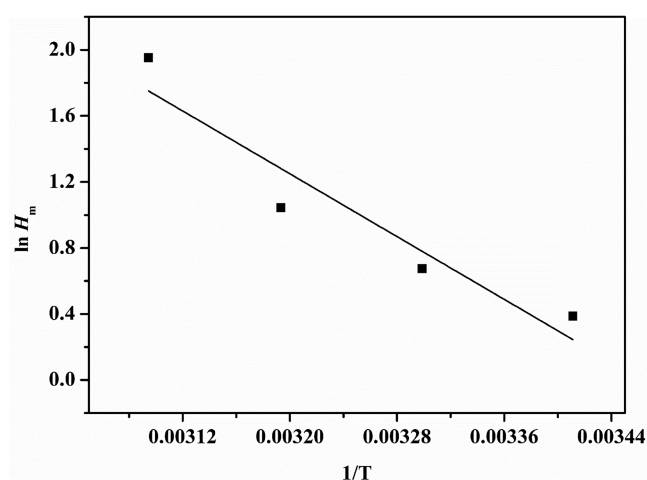
$$\Delta S_{\text{sol}} = \frac{\Delta H_{\text{sol}} - \Delta G_{\text{sol}}}{T} \quad (5)$$

where P^0 refers to the standard pressure (100 kPa). The calculated values of ΔH_{sol} for [EimH][CuCl₂] are -39.5 KJ·mol⁻¹. The values of ΔG_{sol} and ΔS_{sol} are also found to be -1.70 KJ·mol⁻¹ and -124.8 J·mol⁻¹·K⁻¹ at 303.2 K, respectively. Indeed, the value of ΔH_{sol} for [EimH][CuCl₂] is obviously larger than the hydrogen bonding energy (-10 to -20 KJ·mol⁻¹), implying the stronger interaction between CO and [EimH][CuCl₂] and thereby a superior CO absorption capacity.

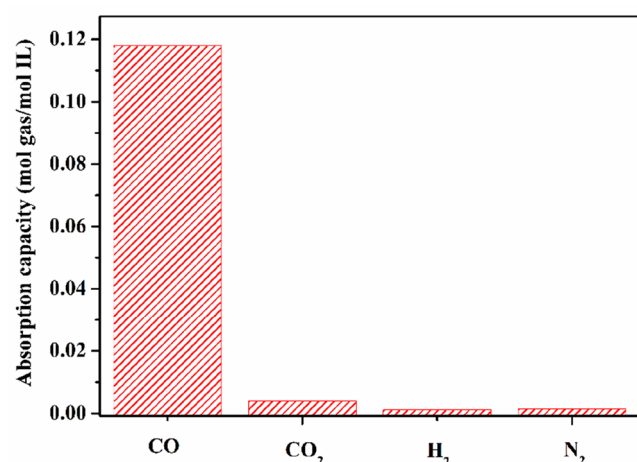
Selectivity of CO Absorption in [EimH][CuCl₂]. Since CO₂, H₂, and N₂ usually exist along with CO in most industrial gas streams, a high selectivity is necessary for selective capture of CO.²⁵ Then the solubilities of pure CO₂, H₂, and N₂ in

Table 2. Henry Constants of CO Absorption in [EimH][CuCl₂]

absorbent	$H_m/100 \text{ kPa}\cdot\text{kg}\cdot\text{mol}^{-1}$			
	293.2 K	303.2 K	313.2 K	323.2 K
[EimH][CuCl ₂]	1.472 ± 0.0049	1.964 ± 0.0019	2.838 ± 0.0020	7.041 ± 0.0049

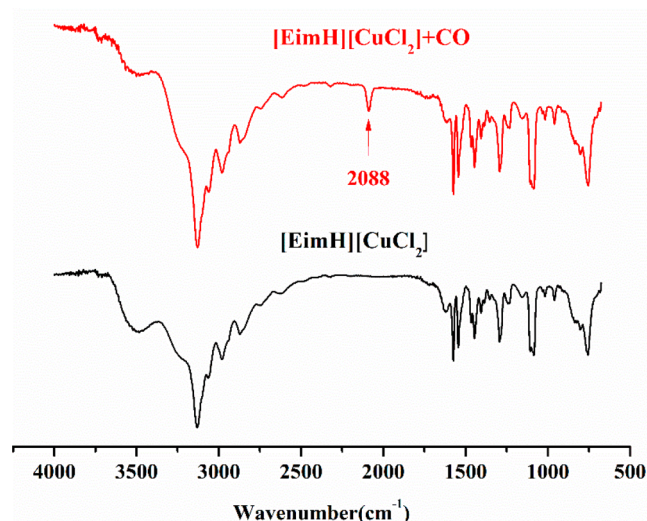
Figure 3. Linear fit of $\ln H_m$ and $1/T$.

[EimH][CuCl₂] were measured at 303.2 K and 1 bar, respectively. It is remarkable that [EimH][CuCl₂] showed very low capacity for capturing pure CO₂, H₂, and N₂ (Figure 4). The ideal selectivities of CO/CO₂, CO/H₂, and CO/N₂ for

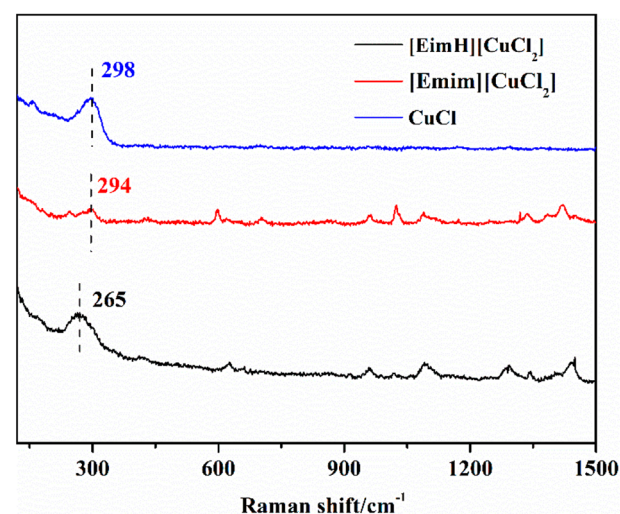
Figure 4. CO, CO₂, N₂, and H₂ absorption in [EimH][CuCl₂] at 303.2 K and 1 bar.

[EimH][CuCl₂] were calculated to be as high as 29.5, 107.2, and 78.7 at 1 bar, respectively. In contrast, the selectivity of CO/CO₂ in the aprotic IL [Emim][CuCl₂] was only 2.17 (Supporting Information, Figure S6). These findings indicate that the PIL [EimH][CuCl₂] displays ultrahigh selectivities for CO capture, showing great potential for selective absorption of CO from CO₂, H₂, and N₂.

Mechanism of CO Absorption in [EimH][CuCl₂]. To clarify great performance of the PIL [EimH][CuCl₂], the interaction between [EimH][CuCl₂] and CO was characterized by infrared (IR) and Raman spectroscopies. In the IR spectra (Figure 5), one new characteristic peak was observed at 2088 cm⁻¹ after CO adsorption, which can be assigned to the

Figure 5. IR spectra of [EimH][CuCl₂] before and after CO capture.

stretching vibration of captured CO. Compared with free CO (2143 cm⁻¹),²⁶ the vibrational frequency of captured CO was slightly red-shifted, related to a relatively strong interaction of [EimH][CuCl₂] with CO. Similarly, the characteristic peak of captured CO was also observed after the absorption of CO in [Emim][CuCl₂] (Figure S7). Moreover, the key role of the protonated imidazolium cation ([EimH]⁺) was further verified by Raman spectroscopy (Figure 6). One should notice a

Figure 6. Raman spectra of [EimH][CuCl₂], [Emim][CuCl₂], and CuCl.

characteristic peak at 298 cm⁻¹ in CuCl, which can be assigned to the stretching vibration of the Cu–Cl bond.²⁷ More importantly, the vibrational frequency of Cu–Cl in the PIL [EimH][CuCl₂] was significantly red-shifted to 265 cm⁻¹, whereas only a very little change was observed in the aprotic IL [Emim][CuCl₂]. The peak appeared at 294 cm⁻¹. This finding

implies that the protonated imidazolium cation in the PIL $[\text{EimH}][\text{CuCl}_2]$ plays a key role in the absorption of CO.

To further uncover the critical role of the protonated imidazolium cation on the enhancement of CO sorption, we performed density functional theory (DFT) calculation with Gaussian 16 at the M06-2x/6-311G++(d,p)/SDD level.²⁸ It has been demonstrated that solutions of CuCl in concentrated HCl can chemisorb CO to form the chloride-bridged complex $[\text{CuCl}(\text{CO})]_2$.²⁹ Our calculation confirmed that the interaction between the isolated $[\text{CuCl}_2]^-$ anion and CO is quite weak ($\Delta H = -8.37$ kJ/mol), while the dimer of the anion, $[\text{Cu}_2\text{Cl}_3]^-$, has more negative sorption enthalpy of -16.73 kJ/mol. Moreover, the results of ESI-MS with negative ion mode (Supporting Information, Figures S1–3) demonstrated that the anions $[\text{CuCl}_2]^-$ and $[\text{Cu}_2\text{Cl}_3]^-$ were detected and coexisted in the PIL $[\text{EimH}][\text{CuCl}_2]$. Thus, it is supposed that the dinuclear copper complex may dominate CO sorption. Then the structures of dimers of PIL $[\text{EimH}][\text{CuCl}_2]$ and aprotic IL $[\text{Emim}][\text{CuCl}_2]$ ion pairs and their complexes with CO are shown in Figure 7. The negative enthalpies of

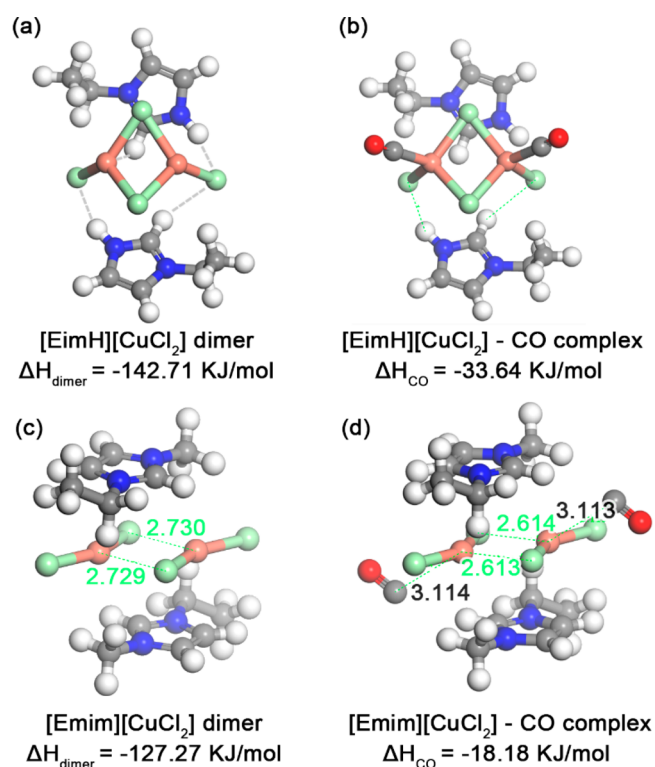


Figure 7. Structures of the dimers of $[\text{EimH}][\text{CuCl}_2]$ and $[\text{Emim}][\text{CuCl}_2]$ pairs and their complexes with CO. (a) Geometry of $[\text{EimH}][\text{CuCl}_2]$ dimer. H-bond network is marked in a gray dashed line. (b) Complex formed by $[\text{EimH}][\text{CuCl}_2]$ and CO. The distance between Cu and neighboring CO is in bold. (c) Geometry of the $[\text{Emim}][\text{CuCl}_2]$ dimer. The lengths of relatively weak bridge Cu–Cl bonds are labeled in green. (d) Complex formed by $[\text{Emim}][\text{CuCl}_2]$ and CO.

dimerization of IL pairs indicate the formation of dimer is energetically favored. For $[\text{EimH}][\text{CuCl}_2]$, the relatively strong N–H⋯Cl hydrogen bond can weaken the terminal Cu–Cl bond, leading to more ligand connecting to Cu^+ , namely, the bridged Cl. As shown in Figure 7a, the bond lengths of terminal and bridge Cu–Cl bonds are 2.310 and 2.439 Å, respectively. Previous experimental and high level ab initio

calculation represented that increasing of coordination number of Cu^+ from 2 to 3 may cause a red-shift of Raman spectroscopy, approximately from 300 to 260 cm^{-1} .³⁰ It is consistent with our observation. Besides, copper and the three connected Cl are not in the same plane, resulting in an unoccupied site for CO coordination. Overall, the adsorption enthalpy is -33.64 kJ/mol. In comparison, for $[\text{Emim}][\text{CuCl}_2]$, without a H bond, the normal Cu–Cl bond in $[\text{CuCl}_2]^-$ is too intense to allow the other Cl-forming bridge bond. Although the linear $[\text{CuCl}_2]^-$ anion bends a little in the dimer, no strong bridge Cu–Cl bond was formed. As a result, the interaction between CO and copper is much weaker, with the enthalpy of -18.18 kJ/mol.

Recycle Test of $[\text{EimH}][\text{CuCl}_2]$. The reusability and stability of an IL is very important for their applications. First, thermogravimetric analysis was performed to test the stability of $[\text{EimH}][\text{CuCl}_2]$ (Supporting Information, Figure S8). It was found that the PIL $[\text{EimH}][\text{CuCl}_2]$ has good stability before reaching the temperature of 450 K. Hence, CO-saturated $[\text{EimH}][\text{CuCl}_2]$ could be heated to 333.2 K under a vacuum of 0.01 bar for 2 h, and there would have been no losses of PIL during desorption. After that, the renewed $[\text{EimH}][\text{CuCl}_2]$ was used for the measurement of CO absorption. The absorption/desorption cycles were performed five times. As shown in Figure 8, the high available absorption

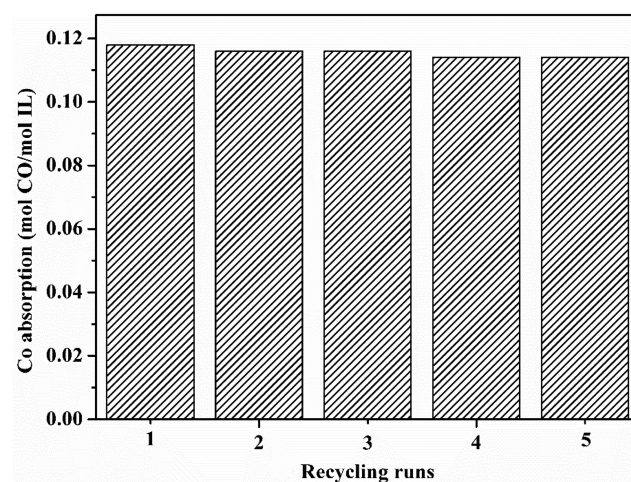


Figure 8. CO absorption/desorption cycles in $[\text{EimH}][\text{CuCl}_2]$.

capacity was well maintained during the five cycles, which indicates good reusability of $[\text{EimH}][\text{CuCl}_2]$ in reversible absorption of CO. It was also found that the IR spectra (Supporting Information, Figure S9) of reused $[\text{EimH}][\text{CuCl}_2]$ after five runs were nearly the same as those of a fresh sample. This implies that the PIL $[\text{EimH}][\text{CuCl}_2]$ is stable enough to be recycled in the absorption of CO.

CONCLUSION

In conclusion, we designed and prepared a class of cuprous-based PILs which exhibit very large absorption capacity for reversibly capturing CO (up to 0.157 mol mol⁻¹ at 293.2 K and 1 bar) and display high selectivities of CO/CO₂, CO/H₂, and CO/N₂. The results of IR and Raman spectroscopies, together with quantum mechanical calculations, demonstrate that compared with the imidazolium cation $[\text{Emim}]^+$ the protonated imidazolium cation ($[\text{EimH}]^+$) played an essential

role in strengthening the ion-pair interaction between CO and dinuclear cuprous species, contributing to such superior CO capacity. We believe that the cuprous-based PILs can be a promising absorbent with great potential application in selective separation of CO.

■ ASSOCIATED CONTENT

📄 Supporting Information

The Supporting Information is available free of charge on the ACS Publications website at DOI: 10.1021/acssuschemeng.9b02540.

Characterization results of cuprous-based PILs, ESI-MS traces, density values, selectivities of CO/CO₂, CO absorption profiles, IR spectra, and thermogravimetric analysis (PDF)

■ AUTHOR INFORMATION

Corresponding Author

*E-mail: djtao@jxnu.edu.cn.

ORCID

Ziqi Tian: 0000-0001-5667-597X

Duan-Jian Tao: 0000-0002-8835-0341

Author Contributions

[†]Y.-M.L. and Z.T. contributed equally to this work.

Notes

The authors declare no competing financial interest.

■ ACKNOWLEDGMENTS

We thank the National Natural Science Foundation of China (21566011, 31570560), the Natural Science Foundation of Jiangxi Province for Distinguished Young Scholars (20162BCB23026), and the Programs of Jiangxi Province Department of Education (GJJ160272) for financial support.

■ REFERENCES

- (1) Friis, S. D.; Lindhardt, A. T.; Skrydstrup, T. The development and application of two-chamber reactors and carbon monoxide precursors for safe carbonylation reactions. *Acc. Chem. Res.* **2016**, *49*, 594–605.
- (2) Chen, D.; Zhao, J.; Zhang, P. F.; Dai, S. Mechanochemical synthesis of metal–organic frameworks. *Polyhedron* **2019**, *162*, 59–64.
- (3) Zhao, J.; Shu, Y.; Zhang, P. F. Solid-state CTAB-assisted synthesis of mesoporous Fe₃O₄ and Au@Fe₃O₄ by mechanochemistry. *Chin. J. Catal.* **2019**, *40*, 1078–1084.
- (4) Zhang, P. F.; Dai, S. Mechanochemical synthesis of porous organic materials. *J. Mater. Chem. A* **2017**, *5*, 16118–16127.
- (5) Hogendoorn, J.A.; van Swaaij, W.P.M.; Versteeg, G.F. The absorption of carbon monoxide in COSORB solutions: absorption rate and capacity. *Chem. Eng. J. Biochem. Eng. J.* **1995**, *59* (3), 243–252.
- (6) Zarca, G.; Ortiz, I.; Urriaga, A. Copper (I)-containing supported ionic liquid membranes for carbon monoxide/nitrogen separation. *J. Membr. Sci.* **2013**, *438*, 38–45.
- (7) Gao, H. S.; Bai, L.; Han, J.; Yang, B. B.; Zhang, S. J.; Zhang, X. P. Functionalized ionic liquid membranes for CO₂ separation. *Chem. Commun.* **2018**, *54*, 12671–12685.
- (8) Chen, F. F.; Huang, K.; Fan, J. P.; Tao, D. J. Chemical solvent in chemical solvent: A class of hybrid materials for effective capture of CO₂. *AIChE J.* **2018**, *64* (2), 632–639.
- (9) Chen, F. F.; Huang, K.; Zhou, Y.; Tian, Z. Q.; Zhu, X.; Tao, D. J.; Jiang, D. E.; Dai, S. Multi-molar absorption of CO₂ by the activation of carboxylate groups in amino acid ionic liquids. *Angew. Chem., Int. Ed.* **2016**, *55* (25), 7166–7170.
- (10) Wang, C. M.; Cui, G. K.; Luo, X. Y.; Xu, Y. J.; Li, H. R.; Dai, S. Highly efficient and reversible SO₂ capture by tunable azole-based ionic liquids through multiple-site chemical absorption. *J. Am. Chem. Soc.* **2011**, *133* (31), 11916–11919.
- (11) Liu, F.; Chen, W.; Mi, J.; Zhang, J. Y.; Kan, X.; Zhong, F. Y.; Huang, K.; Zheng, A. M.; Jiang, L. Thermodynamic and molecular insights into the absorption of H₂S, CO₂, and CH₄ in choline chloride plus urea mixtures. *AIChE J.* **2019**, *65* (5), e16574.
- (12) Huang, K.; Zhang, X. M.; Zhou, L.; Tao, D. J.; Fan, J. P. Highly efficient and selective absorption of H₂S in phenolic ionic liquids: A cooperative result of anionic strong basicity and cationic hydrogen-bond donation. *Chem. Eng. Sci.* **2017**, *173*, 253–263.
- (13) Chen, K. H.; Shi, G. H.; Zhou, X. Y.; Li, H. R.; Wang, C. M. Highly efficient nitric oxide capture by azole-based ionic liquids through multiple-site absorption. *Angew. Chem., Int. Ed.* **2016**, *55* (46), 14364–14368.
- (14) Shang, D. W.; Bai, L.; Zeng, S. J.; Dong, H. F.; Gao, H. S.; Zhang, X. P.; Zhang, S. J. Enhanced NH₃ capture by imidazolium-based protic ionic liquids with different anions and cation substituents. *J. Chem. Technol. Biotechnol.* **2018**, *93*, 1228–1236.
- (15) Ohlin, C. A.; Dyson, P. J.; Laurenczy, G. Carbon monoxide solubility in ionic liquids: determination, prediction and relevance to hydroformylation. *Chem. Commun.* **2004**, No. 9, 1070–1071.
- (16) Anthony, J. L.; Maginn, E. J.; Brennecke, J. F. Solubilities and thermodynamic properties of gases in the ionic liquid 1-*n*-butyl-3-methylimidazolium hexafluorophosphate. *J. Phys. Chem. B* **2002**, *106* (29), 7315–7320.
- (17) Raeissi, S.; Florusse, L. J.; Peters, C. J. Purification of flue gas by ionic liquids: Carbon monoxide capture in [bmim][Tf₂N]. *AIChE J.* **2013**, *59* (10), 3886–3891.
- (18) Gan, Q.; Zou, Y. R.; Rooney, D.; Nancarrow, P.; Thompson, J. L.; Liang, L. Z.; Lewis, M. Theoretical and experimental correlations of gas dissolution, diffusion, and thermodynamic properties in determination of gas permeability and selectivity in supported ionic liquid membranes. *Adv. Colloid Interface Sci.* **2011**, *164* (1–2), 45–55.
- (19) Zarca, G.; Ortiz, I.; Urriaga, A. Kinetics of the carbon monoxide reactive uptake by an imidazolium chlorocuprate (I) ionic liquid. *Chem. Eng. J.* **2014**, *252*, 298–304.
- (20) Tao, D. J.; Chen, F. F.; Tian, Z. Q.; Huang, K.; Mahurin, S. M.; Jiang, D.; Dai, S. Highly efficient carbon monoxide capture by carbanion-functionalized ionic liquids through C-site interactions. *Angew. Chem., Int. Ed.* **2017**, *56* (24), 6843–6847.
- (21) Fry, H. C.; Lucas, H. R.; Narducci Sarjeant, A. A.; Karlin, K. D.; Meyer, G. J. Carbon monoxide coordination and reversible photodissociation in copper (I) pyridylalkylamine compounds. *Inorg. Chem.* **2008**, *47* (1), 241–256.
- (22) Greaves, T. L.; Drummond, C. J. Protic ionic liquids: evolving structure–property relationships and expanding applications. *Chem. Rev.* **2015**, *115* (20), 11379–11448.
- (23) Shang, D. W.; Zhang, X. P.; Zeng, S. J.; Jiang, K.; Gao, H. S.; Dong, H. F.; Yang, Q. Y.; Zhang, S. J. Protic ionic liquid [Bim][NTf₂] with strong hydrogen bond donating ability for highly efficient ammonia absorption. *Green Chem.* **2017**, *19*, 937–945.
- (24) Dong, K.; Zhang, S.; Wang, J. Understanding the hydrogen bonds in ionic liquids and their roles in properties and reactions. *Chem. Commun.* **2016**, *52* (41), 6744–6764.
- (25) Peng, J. J.; Xian, S. K.; Xiao, J.; Huang, Y.; Xia, Q. B.; Wang, H. H.; Li, Z. A supported Cu(I)@MIL-100(Fe) adsorbent with high CO adsorption capacity and CO/N₂ selectivity. *Chem. Eng. J.* **2015**, *270*, 282–289.
- (26) Chavan, S.; Vitillo, J. G.; Groppo, E.; Bonino, F.; Lamberti, C.; Dietzel, P. D. C.; Bordiga, S. CO adsorption on CPO-27-Ni coordination polymer: spectroscopic features and interaction energy. *J. Phys. Chem. C* **2009**, *113* (8), 3292–3299.
- (27) Jiang, B.; Tao, W.; Dou, H.; Sun, Y.; Xiao, X.; Zhang, L.; Yang, N. A novel supported liquid membrane based on binary metal chloride deep eutectic solvents for ethylene/ethane separation. *Ind. Eng. Chem. Res.* **2017**, *56* (51), 15153–15162.

(28) Frisch, M. J.; Trucks, G. W.; Schlegel, H. B.; Scuseria, G. E.; Robb, M. A.; Cheeseman, J. R.; Scalmani, G.; Barone, V.; Mennucci, B.; Petersson, G. A.; Nakatsuji, H.; Caricato, M.; Li, X.; Hratchian, H. P.; Izmaylov, A. F.; Bloino, J.; Zheng, G.; Sonnenberg, J. L.; Hada, M.; Ehara, M.; Toyota, K.; Fukuda, R.; Hasegawa, J.; Ishida, M.; Nakajima, T.; Honda, Y.; Kitao, O.; Nakai, H.; Vreven, T.; Montgomery, J. A. E.; Peralta, J., Jr.; Ogliaro, F.; Bearpark, M.; Heyd, J. J.; Brothers, E.; Kudin, K. N.; Staroverov, V. N.; Kobayashi, R.; Normand, J.; Raghavachari, K.; Rendell, A.; Burant, J. C.; Iyengar, S. S.; Tomasi, J.; Cossi, M.; Rega, N.; Millam, J. M.; Klene, M.; Knox, J. E.; Cross, J. B.; Bakken, V.; Adamo, C.; Jaramillo, J.; Gomperts, R.; Stratmann, R. E.; Yazyev, O.; Austin, A. J.; Cammi, R.; Pomelli, C.; Ochterski, J. W.; Martin, R. L.; Morokuma, K.; Zakrzewski, V. G.; Voth, G. A.; Salvador, P.; Dannenberg, J. J.; Dapprich, S.; Daniels, A. D.; Farkas, O.; Foresman, J. B.; Ortiz, J. V.; Cioslowski, J.; Fox, D. J. *Gaussian 16*, Revision A.03; Gaussian, Inc.: Wallingford, CT, 2009.

(29) Nicholls, D. *Complexes and First-Row Transition Elements*; Palgrave Macmillan: London, 1974; pp 201–206. .

(30) Bolkan, S. A.; Yoke, J. T. Room temperature fused salts based on copper (I) chloride-1-methyl-3-ethylimidazolium chloride mixtures. 1. Physical properties. *J. Chem. Eng. Data* **1986**, 31 (2), 194–197.